Q. 101 – R. 66

COMMISSION INTERNATIONALE
DES GRANDES BARRAGES

VINGT SIXIÈME CONGRÈS
DES GRANDS BARRAGES
Vienne, Juillet 2018

STUDY ON THE MECHANISM OF THE PECULIAR BEHAVIORS OF ARATOZAWA DAM IN THE 2008 EARTHQUAKE*

Nario YASUDA, Norihisa MATSUMOTO
JAPAN DAM ENGINEERING CENTER

Masayoshi NARUOKA
Nuclear Power Eng. Department, ELECTRIC POWER DEVELOPMENT CO., LTD

Zengyan CAO
Senior Engineer, JP BUSINESS SERVICE CORPORATION

JAPAN

SUMMARY

During the 2008 Iwate-Miyagi Earthquake (M7.2) of June 14, 2008, seismic motions with the maximum acceleration of 10.24 cm/s^2 in the stream direction were recorded at the foundation bedrock of Aratozawa dam, a rockfill dam located approximately 16km from the epicenter. However, the maximum response acceleration in the same direction near the center of the dam crest was 5.25 m/s^2, and the acceleration amplification ratio of the dam body was far lower than that normally considered for a rockfill dam. Furthermore, it was measured that the crest settled down 19.8 cm after the earthquake. In this study the dynamical properties of the embankment materials have been identified with the reproduction analysis of the past earthquakes, and the recorded behaviors of the dam body during the mentioned strong earthquake have been simulated. The generating mechanism of the peculiar earthquake behavior has been investigated based on the results of earthquake response analysis. Furthermore, in order to understand

---

* *Étude sur le mécanisme des comportements particuliers du barrage d'Aratozawa durant le tremblement de terre de 2008*

the deformation mechanism, sliding stability analysis and cumulative damage analysis are performed. According to the results, the residual deformation of the dam body after the strong earthquake is inferred to be caused by the shaking settlement of the embankment materials.

RÉSUMÉ

Lors du tremblement de terre d'Iwate-Miyagi (M7.2) du 14 juin 2008, des mouvements sismiques avec une accélération maximale de 10,24 m/s^2 dans le sens du courant ont été enregistrés sur les fondations du barrage d'Aratozawa, un barrage en enrochement situé à environ 16 km de l'épicentre. Cependant, l'accélération de la réponse maximale dans la même direction près du centre de la crête du barrage était de 5,25 m/s^2, et le rapport d'amplification de l'accélération du corps du barrage était bien inférieur à celui normalement considéré pour un barrage en enrochement. De plus, il a été mesuré que la crête se stabilisait à 19,8 cm suite au tremblement de terre. Dans cette étude, les propriétés dynamiques des matériaux de remblai ont été identifiées grâce à l'analyse de reproduction des tremblements de terre passés, et les comportements du corps du barrage enregistrés lors du grand séisme ont été simulés. Le mécanisme de génération des comportements sismiques particuliers a été étudié en fonction des résultats de l'analyse de réponse aux tremblements de terre. En conséquence, afin de comprendre le mécanisme de déformation, une analyse de stabilité de glissement et une analyse des dégâts cumulatifs ont été effectuées. Selon les résultats, la déformation résiduelle du corps du barrage après le grand tremblement de terre est supposée être causée par la secousse des matériaux du remblai.

Keywords: finite element method, rockfill dam, seismic resistance.

1. INTRODUCTION

Seismic design of embankment dams in Japan is done with the seismic coefficient method using a constant design seismic coefficient stipulated empirically for each region, based on the Cabinet Order concerning Structural Standards for River Management Facilities, etc. and the Ministry of Land, Infrastructure, Transportation and Tourism Ordinance for Structural Standard for River Administration Facilities. In the guideline for seismic design of embankment dams (1991), the maximum ground seismic coefficient is stipulated as 0.15 even in a strong seismic region, provided that a safety margin is ensured. But after The 1995 Kobe Earthquake, with the improvement of the earthquake monitoring system, a number of earthquake records far stronger than the design seismic coefficients of the dams have

been obtained, for example, the 2000 Tottori Earthquake, the 2004 Mid Niigata Earthquake, the 2008 Iwate-Miyagi Earthquake, and the 2011 Tohoku Earthquake. Examining the earthquake behaviors of the embankment dams subjected to strong earthquakes with numerical methods, furthermore studying the deformation or damage mechanism would be extremely beneficial for the seismic design of new dams and the seismic safety assessment of existing dams.

Aratozawa dam is a 74.4 m high rockfill dam with central clay core completed in 1998. When the 2008 Iwate-Miyagi Earthquake struck, seismic motion with the maximum acceleration 10.24 m/s^2 was recorded in the dam foundation. On the other hand, the maximum acceleration response in the stream direction near the center of the dam crest was 5.25 m/s^2. The acceleration amplification ratio of the dam body was 0.51, which is far lower than that recorded previously in other rockfill dams. After the earthquake, a survey on the dam was made [1]. It was measured that the crest settled about 19.8 cm relative to the original status about half year ago.

In this research, 3-D equivalent linear analysis is performed to simulate the earthquake behaviors of Aratozawa dam in order to clarify the generating mechanism of aforementioned phenomenon. Based on the results of the earthquake response analysis, sliding stability analysis and cumulative damage analysis were carried out to reason out the mechanism of the residual deformation induced by the earthquake.

2. DAM SPECIFICATIONS AND EARTHQUAKE MONITORING

2.1. Dam specifications

Table 1 shows the main features of Aratozawa dam. Fig. 1 shows the plan view and the typical cross section of the dam body. The locations of the seismographs are also marked in the same figure. Seismographs were installed in the dam foundation (F), its middle of the center core (M), dam crest (T) and the right abutment (G) in the three directions (stream, cross stream and vertical directions).

2.2. Recorded seismic motions during the 2008 Iwate-Miyagi earthquake

On June 14, 2008, the 2008 Iwate-Miyagi Earthquake (M7.2) occurred with its epicenter only 16km away from Aratozawa dam. Fig. 6 shows the acceleration

records of the dam foundation (F), the middle of the center core (M), and the dam crest (T). The maximum acceleration of 10.24 m/s^2 was recorded in the stream direction in the foundation bedrock. While the maximum accelerations in the same direction in the middle of the center core and the dam crest were 5.35 m/s^2 and 5.25 m/s^2 respectively. As the earthquake records in the dam foundation this is the largest one recorded in Japan up to now.

By a survey [1] conducted on June 30 of the same year (i.e. 16 days after the main shock), a settlement of about 19.8 cm at the dam crest and a residual deformation of 4.3 cm toward the upstream side and 6.0 cm in the cross stream direction were measured. It should be noticed that these displacements are the increments since December 4, 2007 and include the deformation caused by many aftershocks.

Table 1
Main features of Aratozawa dam

Dam location	Aratozawa, Miyagi Prefecture
Dam type	Rockfill dam with central clay core
Dam height	74.4m (Lowest ground elevation: EL205.0m)
Crest length	413.7m
Crest width	10.0m
Crest elevation	EL.279.4m
Slope gradients	Upstream: 1:2.7 Downstream: 1:2.1
Dam volume	3,048,000 m^3
Basin area	20.4 km^2
Reservoir capacity	13,850,000 m^3
Design seismic coefficient	0.15 (dam body), 0.18 (intake tower, bridge) 0.16 (spillway)

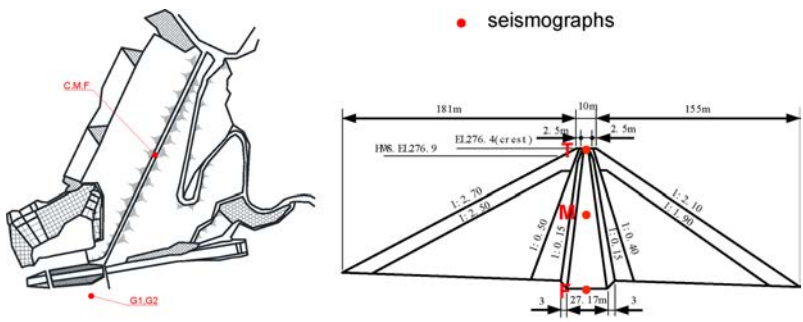

Fig. 1
Locations of seismographs at Aratozawa dam
Emplacements des sismographes au barrage d'Aratozawa

3. REPRODUCTION ANALYSIS OF THE EARTHQUAKE BEHAVIORS

3.1. Analysis procedure

In order to investigate the mechanism of the acceleration decrement in the dam body during the mentioned earthquake, an earthquake response analysis is carried out with the 3-D equivalent linearization method. The reference shear strain and the maximum damping coefficient are identified by adjusting these factors for getting the analysis results most similar to the earthquake records. The consistency between the analysis results and the earthquake records is evaluated, focusing on the values of the maximum acceleration response, acceleration wave forms, Fourier spectra, and transfer functions between the positions of the seismographs. The input earthquake motions are reproduced by pulling back the recorded seismic motions of the foundation to the bottom of the analysis model (base of bedrock) by the 3-D transfer function method, which will be described in the next section.

Fig. 2 shows the flow chart of analysis procedure. A specialized code for the earthquake response analysis of dams, named "Universe" is used in the analysis. As for the mechanism of the residual deformation of the dam due to earthquake, it will be mentioned in the next chapter.

3.2. Analysis conditions

3.2.1. Analysis model

The 3-D analysis model shown in Fig. 3 is made based on the design drawings of the dam body and detailed topographical data of the dam site. At the boundaries around and beneath the foundation viscous boundary condition [2] is applied, which has much better energy absorption function than the conventional one [3]. The initial effective stress of the dam body with the reservoir water level of 270.1 m during the earthquake is calculated with the consideration of seepage pressure. Because of the uncertainty concerning the effects of the excessive pore water pressure in the dam it is ignored in the earthquake response analysis. i.e., the analysis is done with the total stress method.

3.2.2. Material properties

The equivalent linearization method is used to consider the effects of the nonlinear properties of the embankment materials during the earthquake. The shear strain dependency of the shear modulus and the damping coefficient are set with the hyperbolic model of Eq. [1] and Eq. [2].

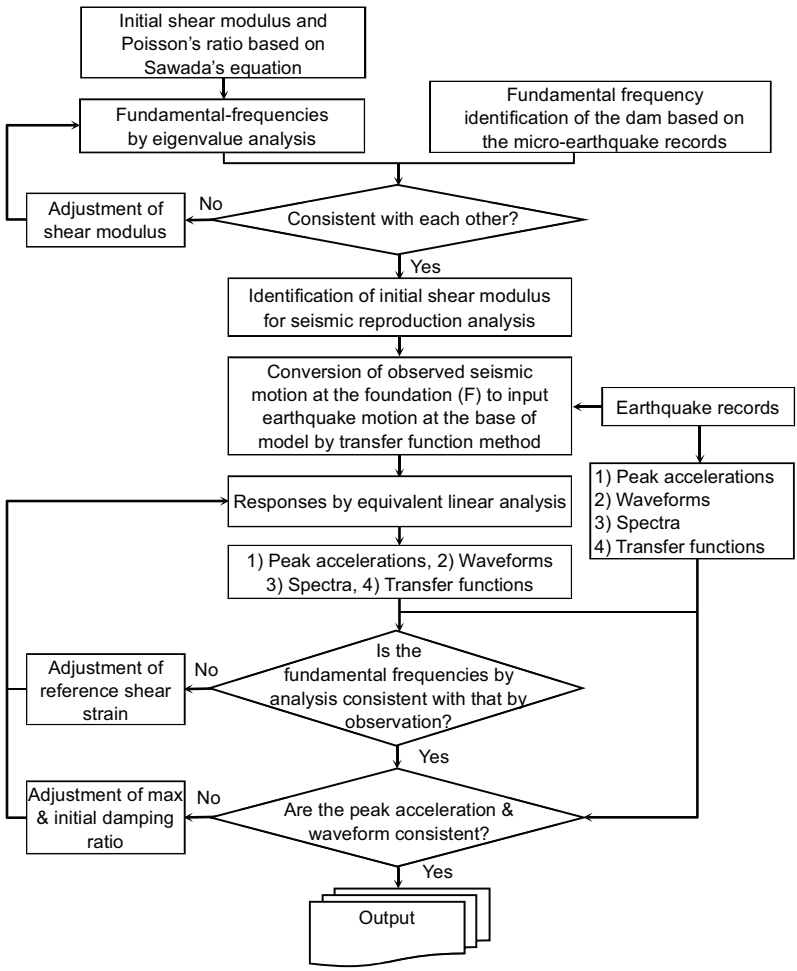

Fig. 2
Flow chart of reproduction analysis
Diagramme d'analyse de reproduction

$$\frac{G}{G_0} = \frac{1}{1+\gamma/\gamma_r} \qquad [1]$$

$$h = h_{\max}\frac{\gamma}{\gamma+\gamma_r} + h_0 \qquad [2]$$

where G and G_0 represent the equivalent shear modulus and its initial value. h, h_0, and h_{max} represent the equivalent damping coefficient, its initial value and its maximum value respectively. γ represents the effective shear strain (2/3 of its maximum value), and γ_r represents the reference shear strain. While in the reproduction analysis, γ_r is adjusted as one of the identification parameters as mentioned in Fig. 2.

The initial shear modulus G_0 of the embankment materials in the analysis is set based on the Sawada's equation [4]. But it is modified by eigenvalue analysis in order that the fundamental frequency got from the analysis conforms to that estimated according to the transfer function obtained from the past earthquake records. It is assumed that the initial damping coefficient of the embankment materials at the small strain level is uniformly 5%. In order to improve the reproducibility of earthquake responses, the maximum damping coefficient is modified.

Furthermore, the material damping is evaluated as Rayleigh's type damping with the following formula.

$$[C]^e = \alpha[M]^e + \beta[K]^e \qquad [3]$$

where $[C]^e$, $[M]^e$ and $[K]^e$ represent damping, mass and stiffness matrices of each finite element respectively.α and β are parameters defined by the following formulae.

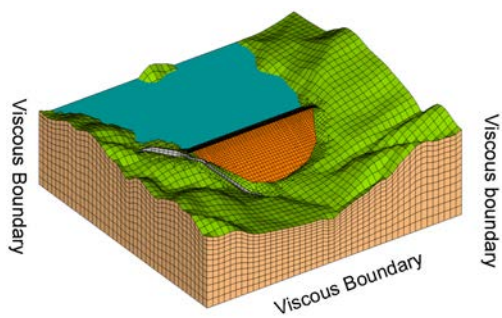

Fig. 3
Analytical Model
Modèle analytique

$$\alpha = 1.4 \cdot h \cdot \omega_1 \qquad \beta = 0.6\,h/\omega_1 \qquad [4]$$

where ω_1 represents the fundamental circular frequency of the dam body.

The shear modulus of the spillway concrete is assumed to be 12,500 N/mm^2, which is the general value of the dam concrete. The shear modulus of the foundation bedrock is set to be 5,500 N/mm^2, obtained by conversion from the shear wave velocity 1,440 m/s of the CM class rock (Index of rock property in Japan). The Poisson's ratios of the embankment materials are set based on the Sawada's equation.

The densities of the embankment materials used for the analysis are shown in Table 2, which are the material test results for the quality control of the dam construction.The Poisson's ratio of the spillway is 0.2 as concrete material, and that of the foundation bedrock is set to be 0.25.

Table 2
Densities of the embankment materials, spillway and foundation bedrock

MATERIAL CATEGORY		DENSITY(G/CM^3)	
		WET	SATURATED
Core		2.04	2.10
Filter		2.34	2.43
Transition		2.24	2.33
Upstream rock	Inner	2.15	2.29
	Outer	2.15	2.32
Downstream rock	Inner	2.18	2.32
	Outer	2.13	2.30
Spillway		2.40	
Foundation bedrock		2.60	

3.2.3. Input earthquake motion

In the analysis, the input earthquake motion is prepared by pulling back the earthquake records of the foundation (Point F in Fig. 4) to the bottom surface of the analysis model using a 3-D wave transfer function method. The core of the method is how to find the transfer function of the foundation model. The image of the method is shown in Fig. 4, and it can be described in the followings.

Step 1: To get the responses of the foundation (Point F)

3-D earthquake response analysis is performed with the dam – reservoir – foundation model where the water level is set at that during the earthquake (270.1m). In the analysis, the earthquake records of the foundation (Point F) are used as the input earthquake motion to the bottom boundary, but the 3 directional components are inputted separately. Hence, 3 sets of response results are obtained and named as,

$$\begin{cases} \{R_{xx},\ R_{yx},\ R_{zx}\} & When\ \ W_{Fx}\ \ is\ \ inputted \\ \{R_{xy},\ R_{yy},\ R_{zy}\} & When\ \ W_{Fy}\ \ is\ \ inputted \\ \{R_{xz},\ R_{yz},\ R_{zz}\} & When\ \ W_{Fz}\ \ is\ \ inputted \end{cases} \quad [5]$$

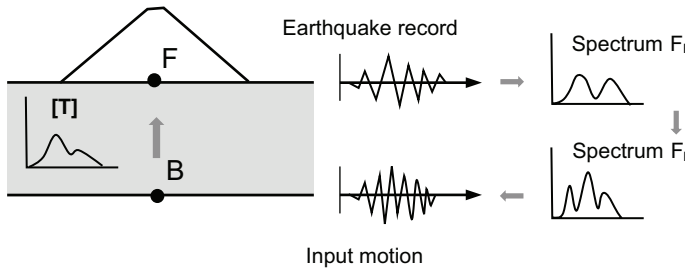

Fig. 4
Reproduction of input earthquake motion
Reproduction de mouvement de tremblement de terre d'entrée

where $R_{ij}\left(i,j=x,y,z\right)$ indicates the response of Point F, and $W_{Fi}\left(i=x,y,z\right)$ indicates the earthquake motions recorded at Point F.

Step 2: To get the input earthquake motions of bottom boundary (Point B)

The Fourier spectra $F_{WFi}\left(i=x,y,z\right)$ of the input earthquake motions W_{FX}, W_{FX}, W_{Fy}, W_{Fz} and those of the responses at Point F $F_{Rij}\left(i,j=x,y,z\right)$ are obtained, and then the transfer functions $T_{ij}\left(i,j=x,y,z\right)$ of the foundation can be got with the following equations.

$$\begin{aligned}
T_{xx}&=\frac{F_{R_{xx}}}{F_{W_{Fx}}},\ T_{yx}=\frac{F_{R_{yx}}}{F_{W_{Fx}}},\ T_{zx}=\frac{F_{R_{zx}}}{F_{W_{Fx}}}\\
T_{xy}&=\frac{F_{R_{xy}}}{F_{W_{Fy}}},\ T_{yy}=\frac{F_{R_{yy}}}{F_{W_{Fy}}},\ T_{zy}=\frac{F_{R_{zy}}}{F_{W_{Fy}}}\\
T_{xz}&=\frac{F_{R_{xz}}}{F_{W_{Fz}}},\ T_{yz}=\frac{F_{R_{yz}}}{F_{W_{Fz}}},\ T_{zz}=\frac{F_{R_{zz}}}{F_{W_{Fz}}}
\end{aligned} \qquad [6]$$

Then, the Fourier spectra $F_{WBi}\left(i=x,y,z\right)$ of the input earthquake motion at the bottom boundary of the foundation are got with the Eq. [7].

$$\begin{Bmatrix} F_{W_{Fx}} \\ F_{W_{Fy}} \\ F_{W_{Fz}} \end{Bmatrix} = \begin{bmatrix} T_{xx} & T_{xy} & T_{xz} \\ T_{yx} & T_{yy} & T_{yz} \\ T_{zx} & T_{yz} & T_{zz} \end{bmatrix} \begin{Bmatrix} F_{W_{Bx}} \\ F_{W_{By}} \\ F_{W_{Bz}} \end{Bmatrix} \qquad [7]$$

By inverse Fourier transformation of the spectra F_{WBX}, F_{WBY} and F_{WBZ}, the input earthquake motions $W_B^1\left(W_{Bx}^1,\ W_{By}^1,\ W_{Bz}^1\right)$ at the bottom of the

foundation model are reproduced. And the superscript 1 of W_B^1 indicates the first estimation.

Step 3: To improve the accuracy of the input earthquake motions

In order to improve the accuracy of the estimated input earthquake motion, above procedure is repeated because of the nonlinearity of the embankment materials. In the response analysis of Step 1 of the first estimation, the dam body is treated as linear material. Therefore, the response analysis of Step 1 is performed again with the equivalent linearization method and by inputting the earthquake $W_{Bi}^1(i = x, y, z)$, instead of $W_{Fi}(i = x, y, z)$. Then the Step 2 is repeated with a more accurate of the transfer functions $T_{ij}(i, j = x, y, z)$, and a more accurate estimation of the input earthquake motion W_B^2 is got and used in the earthquake behavior reproduction analysis.

3.3. Reproduction analysis results

3.3.1. Identified reference shear strain and the maximum damping coefficient

The reproducibility of the earthquake behavior is examined by comparing the reproduction analysis results and the earthquake records, focusing on the values of the maximum acceleration responses, response wave forms, Fourier spectra and the acceleration transfer functions of the dam body.

The reference shear strain and the maximum damping coefficient of the embankment materials are repeatedly modified for getting higher reproducibility. As a result, in the case shown in Fig. 5 and Table 3, the earthquake response of the dam body is thought to be consistent generally with the earthquake records. Therefore, it is assumed that the material properties shown in Table 3 reflect the state of the actual dam. And in general, these identified physical values conform to the results of the past laboratory material tests [5], [6], [7].

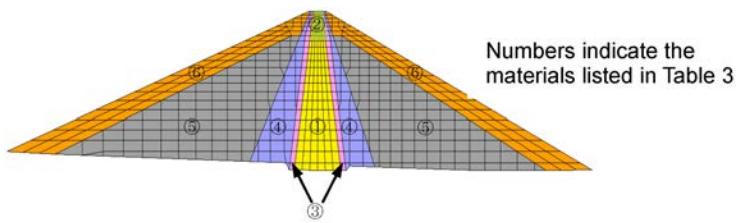

Fig. 5
Zoning of dam body
Zonage du corps du barrage

Table 3
Identified reference shear strain and the maximum damping coefficient

CATEGORY	THE MAX. DAMPING COEFFICIENT h_{max}	REFERENCE SHEAR STRAIN γ_r
① Core (middle & lower)	20%	3.0×10^{-4}
② Core (surface)	30%	
③ Filter ④ Transition	30%	4.0×10^{-4}
⑤ Rock (inner) ⑥ Rock (outer)	23%	

3.3.2. Acceleration response

Table 4 summarizes the values of the maximum acceleration and the relative displacement response of the reproduction analysis and the earthquake records. The fundamental frequency of the dam got by the analysis and earthquake record is also listed in the table. Figs. 6(1) to 6(3) shows the acceleration response histories of each position of the seismographs. Fig. 7, as an example, compares the Fourier spectra and the transfer functions of the acceleration responses at the dam foundation and the crest in the stream direction.

Table 4
The maximum responses of the dam body

ITEM	POSITION	DIRECTION	RECORD	ANALYSIS
Max. acceleration (m/s^2)	Dam crest(T)	Stream	+5.10 -5.25	+6.80 -5.44
		Cross stream	+4.55 -4.37	+6.14 -4.72
		Vertical	+4.88 -6.22	+4.48 -4.72
	Middle of the center core(M)	Stream	+4.02 -5.35	+3.27 -3.04
		Cross stream	+4.78 -3.80	+2.72 -2.58
		Vertical	+4.46 -4.70	+3.08 -4.2
	Foundation(F)	Stream	+10.24 -6.73	+9.93 -5.46
		Cross stream	+8.99 -7.13	+8.68 -6.24
		Vertical	+6.91 -6.14	+5.61 -5.24
Fundamental frequency (stream direction (Hz))			1.47	1.47
Relative displacement of the crest to the foundation in stream direction (cm)			+11.13 -1.76	+7.72 -11.58

As shown in Table 4 and Fig. 6, although there is some discrepancy in the values of the maximum acceleration at each position between the analysis results and the earthquake records, the acceleration response waveforms generally conform each other. Good reproducibility is obtained throughout the entire time histories of the acceleration responses at the foundation and the middle of the central core in particular. In those of the crest, during the first 4 seconds from the beginning both the recorded waves and those got from the analysis

show almost identical phases, or else the peaks of the recorded waves appear slightly faster than those of the analysis. While in the later histories, to the contrary, the responses based on the analysis appear to transmit more quickly than the recorded ones. As the reason for this, it is thought that the stiffness of the embankment material in analysis is a constant value throughout the whole time history (equivalent linearization method). In contrast, in the actual dam, it is thought that due to the major motion of the earthquake, the increment of the shear strain response induced the decrement of the embankment material's stiffness. Accordingly, the seismic motion transmission velocity gets down. From Fig. 7, it can be found that, in the low frequency domain up to about 2 Hz, both the Fourier spectra and the transfer functions obtained from the earthquake records and analysis results conform closely each other. As the frequency becomes higher, the difference between records and analysis becomes large gradually. It is presumed that the material properties, i.e., the shear modulus and damping coefficient evaluated according to the maximum shear strain are proper for the low frequency domain. Consequently, the same material property brings relative large error to the response of the higher frequency components.

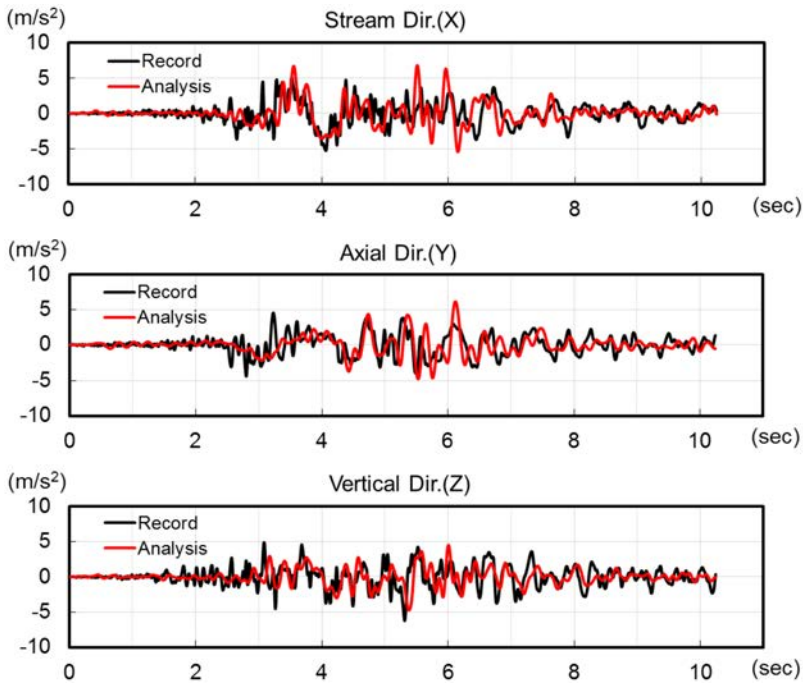

Fig. 6(1)
Time histories of acceleration response, Crest (T)
Diagramme de temps de réponse d'accélération, créte (T)

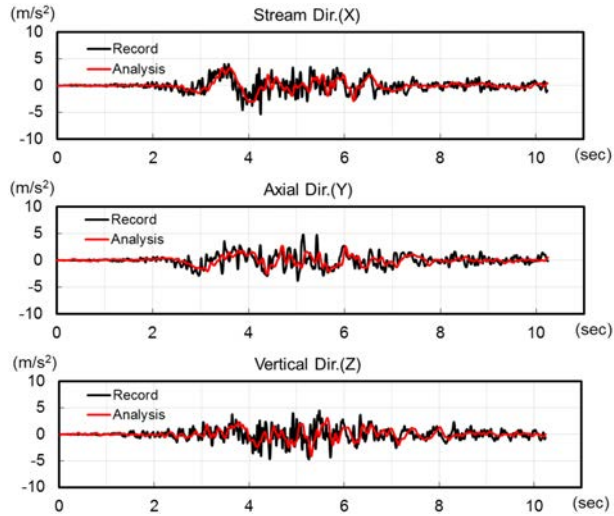

Fig. 6 (2)
Time histories of acceleration response, Middle of core (M)
Diagramme de temps de réponse d'accélération, milleu du noyan (M)

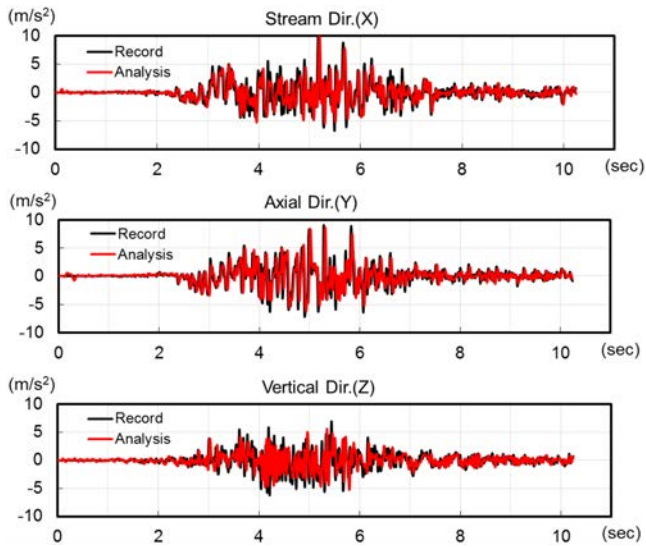

Fig. 6 (3)
Time histories of acceleration response, Foundation (F)
Diagramme de temps de réponse d'accélération, fondation (F)

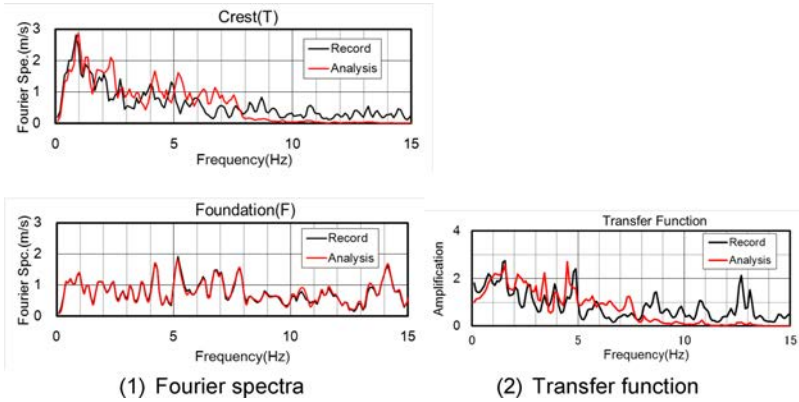

Fig. 7
Fourier spectra and transfer function
Spectre de Fourier et fonction de transfert

3.4. DISPLACEMENT RESPONSE

Fig. 8 shows the response history of the relative displacement of the dam crest to the foundation in the stream direction. The relative displacement obtained by integrating the earthquake records is also shown in the same figure. The maximum relative displacement in the stream direction is about 11 cm (half-amplitude). It is clear that relatively large displacement occurred in the dam body during the earthquake. This large relative displacement is mainly the contribution of the vibration component of a period of 1 second or longer between the time of 3 seconds and 4 seconds of the acceleration records. With the displacement response, it can be presumed that large shear strain occurred in the dam body (average shear strain is about 1.48×10^{-3} (relative displacement/dam height)).

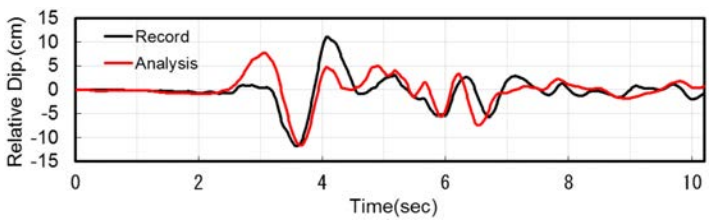

Fig. 8
Displacement in the stream direction of the dam crest relative to the foundation
Déplacement dans la direction du flux de la crête du barrage par rapport à la fondation

3.5. Investigation on the mechanism of peculiar acceleration response

Fig. 9 shows the distribution of the maximum acceleration response in the stream direction obtained by reproduction analysis. The greatest feature of this figure is that the acceleration response is decaying sharply through the rock surface. In addition, the amplification of the acceleration is very light near the crest and the slope surfaces. Near the contact surface with foundation rock, the contrast of the stiffness of the embankment materials and the foundation rock was large. It is presumed that a large phase difference occurred between these two kinds of media due to the major motion of the earthquake. As a result, large shear strain occurred at the bottom of the rock zone (see Fig. 10). Consequently, the shear modulus of the embankment materials greatly decreased and their damping became larger. It is presumed that the acceleration response at the middle of the core zone was drastically attenuated due to such reasons.

Near the crest and in the slope surface layers, shear strain increased due to the major motions of the earthquake (see Fig. 10). The embankment materials

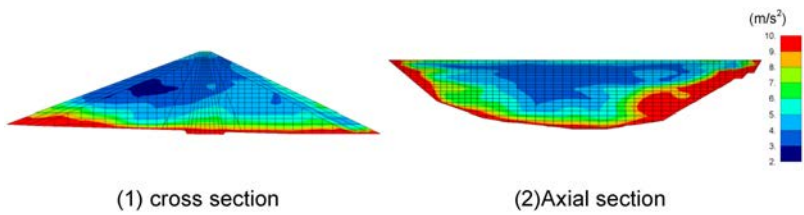

Fig. 9
Maximum acceleration response distribution in the stream direction
Distribution de réponse d'accélération maximale dans la direction du flux

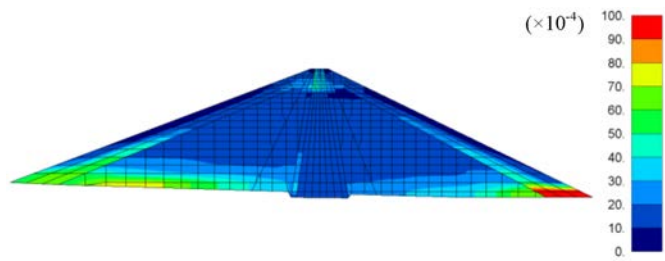

Fig. 10
Distribution of the maximum shear strain
Distribution du cisaillement maximum

of these parts became loose (as a result, the stiffness decreased and the damping increased). Therefore, it is presumed that the amplification of the acceleration response to the comparatively high frequency components of the earthquake became difficult. The almost complete lack of high frequency component after the major motions in the recorded acceleration response at the dam crest as shown in Fig. 6 also supports this speculation. It is inferred that these factors caused the phenomenon of the reversal relationship of the acceleration response at the dam crest and the foundation of the dam during the earthquake.

4. ANALYSIS OF THE RESIDUAL DEFORMATION

As aforementioned, after the 2008 Iwate-Miyagi Earthquake the maximum settlement of 19.8 cm was measured at the crest of Aratozawa dam. This field survey was conducted 16 days after the main shock, so the measured residual deformation included the displacement by many aftershocks. Furthermore, the measured value of 19.8 cm is an increment from December 4 of 2007, so it is impossible to accurately confirm the quantity of residual deformation caused by only the main shock.

However, it is assumed that a high percentage of the measured residual deformation of the dam body was caused by the main shock of the 2008 Iwate-Miyagi Earthquake. In this study, even if it is qualitative, the mechanism of the residual deformation is investigated.

4.1. Analysis method

The residual deformation of a rockfill dam induced by an earthquake is considered to include two kinds of components. One is that caused by sliding behavior and the other is that caused by shaking subsidence of the embankment materials during the earthquake (cumulative damage). For this study, the earthquake response of the dam body obtained by the reproduction analysis described in the previous sections is used

(1) to calculate sliding deformation and
(2) to analyze cumulative damage.

The mechanism of residual deformation of the dam body is investigated by checking which kind the measured residual deformation is.

4.2. Sliding calculation

The sliding calculation of the typical cross-section of the dam body as shown in Fig. 5 is carried out with the Watanabe and Baba method [8].

In order for the sliding arcs to cover the entire dam body, they are divided into a case of sliding on the upstream side of the dam and a case of sliding on the downstream side of the dam (total of 1,235 arcs). The sliding arcs on the upstream side are further divided into those with both ends passing through only the upstream surface (called the "U1 Group"), those with the upper end passing through the crest and the lower end through the upstream surface (called the "U2 Group"), and those with the upper end passing through the downstream surface and the lower end through the upstream surface, i.e., cutting the core zone (called the "U3 Group"). The sliding arcs on the downstream surface are similarly divided into "D1 Group", "D2 Group", and "D3 Group". As an example, Fig. 11(1) shows the arcs for the case of sliding on the upstream side through the crest (in other words, U2 Group).

Of the sliding arc groups, the arcs with the smallest sliding safety factors are abstracted and summarized in Table 5. Fig. 11(2) shows the locations of the corresponding sliding arcs. Focusing on the arcs with sliding safety factors less than 1.0, the sliding displacements are calculated as shown on Table 5. The minimum sliding safety factor is 0.839 on the Arc No.1, a limited part of the upstream surface. But its sliding displacement is almost zero (0.0006 cm). This result suggests that sliding behavior did not occur during the 2008 Iwate–Miyagi Earthquake at Aratozawa dam, and the residual deformation measured after the earthquake was not caused by sliding.

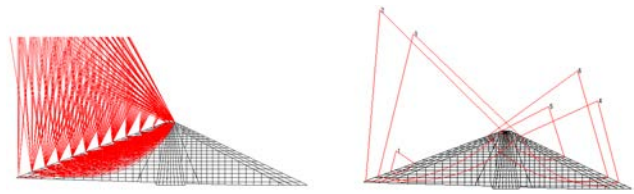

Fig. 11
Sliding calculation
Calcul du glissement

Table 5
Sliding calculation results

SLIDING DIRECTION	ARC GROUP	ARC NO.	SAFETY FACTOR	SLIDING DISPLACEMENT (CM)
Upstream side	U1	1	0.839	0.0006
	U2	2	2.027	–
	U3	3	2.395	–
Downstream side	D1	4	2.581	–
	D2	5	2.090	–
	D3	6	2.135	–

4.3. CUMULATIVE DAMAGE ANALYSIS

It has been pointed out that subjected to intensive seismic motions, the residual deformation of a rockfill dam may be caused by the shaking subsidence of the embankment materials [9]. Such cumulative deformation can be simply evaluated by assuming that it was caused by a decline of stiffness, performing static dead-weight analysis using the shear moduli of the dam body before and after the earthquake. Here, using the initial shear moduli of the dam body and those obtained by the equivalent linear analysis in Section 3, the deformation calculation based on dead-weight analysis is performed. The difference between the deformation results after and before the earthquake is regarded as residual deformation caused by the earthquake. In short.

$$U_r = U_a - U_b \qquad [8]$$

where, U_r is the residual deformation caused by the earthquake. U_a and U_b are the deformation by dead-weight analysis after and before the earthquake respectively.

Fig.12(1) shows the calculated residual deformation of the dam body. The contours show the quantity of settlement on the downstream side. Fig. 12(2) shows the settlement of the dam in the axial section. The maximum settlement is 6.81 cm which occurred near the right abutment. At the crest of the largest cross section of the dam body, the settlement is about 4.26 cm. For the reason mentioned above, the calculation results of the residual deformation cannot be quantitatively compared with the values measured before and after the earthquake. However, based on this calculation result it can be inferred that subjected to the main shock, shaking settlement of the embankment materials caused the residual deformation of the dam body.

Fig. 13 compares the calculated settlement strain with the measured one along the center of the core zone. Both the calculation and measurement show small strain below the elevation of 245 m. Above this elevation, the settlement

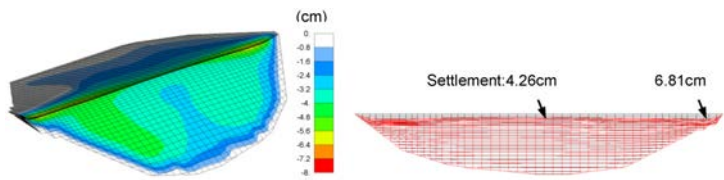

Fig. 12
Residual deformation
Déformation résiduelle

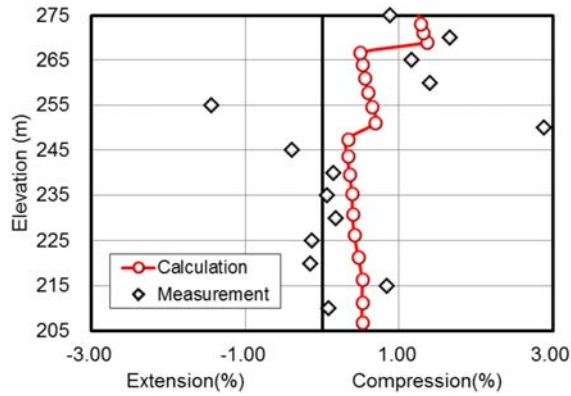

Fig. 13
Comparison on settlement strain (period: Dec.4, 2007 to June 17, 2008)
Comparaison sur la contrainte de règlement (période: du 4 décembre 2007 au 17 au juin 2008)

strain fluctuated wildly and the value is relatively large. For this reason, it is inferred that residual deformation of the dam body after the earthquake was primarily due to the settlement at the higher elevation of the dam body down to a depth of 30 m from the crest. Similarly to the aforementioned residual deformation, the measured settlement strain is also the increment since December 4 of 2007, preventing a quantitative comparison. But, clearly, the distribution tendency of the calculated settlement strain and the measurement results generally conform even in the depth direction.

From the above, it is inferred that the measured residual deformation of the dam body was caused not by sliding behavior of the dam body, but by shaking settlement of the embankment materials.

5. CONCLUSION

From above study, following conclusions can be drawn.

The mechanism that caused the peculiar damping phenomenon (amplification ratio: 0.5) of the acceleration response in Aratozawa dam during the 2008 Iwate-Miyagi Earthquake is examined. Subjected to the major motions of the earthquake, large shear strain occurred near the rock contact surface. Such shear strain response reduced the stiffness, at the same time, increased the damping of the embankment materials. This caused the seismic motions to attenuate immediately near the rock contact surface. Furthermore, near the crest and the slope surface

layers, the major motions of the earthquake caused the embankment materials to loosen. This variation restrained the response to the high frequency components of the earthquake motions. Therefore, the amplification of the acceleration at the crest and the slope surface is very small. It is drawn that these two points caused the reversal of the magnitude of the acceleration response at the crest and the foundation bedrock during this earthquake.

The generating mechanism of residual deformation of the dam body caused by the 2008 Iwate-Miyagi Earthquake is investigated by sliding calculation and the cumulative damage analysis. It is confirmed that sliding phenomenon did not occur during this earthquake. It is also inferred that the residual deformation after the earthquake was caused mainly by shaking settlement of the embankment materials. The settlement strain is large to the depth of about 30m from the crest, and it is deduced that the measured residual deformation was caused primarily by the settlement of the upper part of the dam body.

ACKNOWLEDGEMENTS

The earthquake records provided by Japan Commission on Large Dams (JCOLD) for this research are gratefully acknowledged. The authors wish to acknowledge the Miyagi Prefecture for preparing the materials of Aratozawa dam. This research was also guided by advice given by Dr. Sasaki of the River Department of the National Institute for Land and Infrastructure Management, and by Mr. Sato of the Hydraulic Engineering Research Group of the Public Works Research Institute. And Mr. Sato and Mr. Asaka of the Social & Environmental Engg. Dept., JP Business Service Corporation provided generous advice and assistance with the reproduction analysis of the earthquake behavior. The authors are deeply grateful to them for their contribution.

REFERENCES

[1] SHIMAMOTO K., SATO N., OHMACHI T., KAWASAKI H., IWAI S. "Report on survey of damage to dams by the 2008 Iwate – Miyagi Earthquake", 2009 (in Japanese)

[2] MIURA F., OKINAKA H. Dynamic Analysis Method for 3-D Soil-Structure Interaction Systems with the Viscous Boundary Based on the Principle of Virtual Work, *Proc. of JSCE,* No.404/I-11, April, 1989 (in Japanese)

[3] LYSMER, J., KUHLEMEYER, R. L. Finite dynamic model for infinite media, *Proc. ASCE, EM 4*, pp.859-877, 1969

[4] SAWADA, Y., TAKAHASHI, T. Study on the material properties and the earthquake behaviors of rockfill dams, *Proc. of the 4th Japan Earthquake Engineering Symposium,* pp.695-702, 1975

[5] YASUDA M., OGATA N., SHIMADA, M. Dynamic deformation properties of core materials according to vibration triaxial testing, *Proc. of the 14th Conference on Soil Engineering Research,* 1980

[6] BABA, K., WATANABE, H. On a Consideration for an Earthquake-resistant Design Method for Rockfill Dams, *13th Congress on Large Dams,* New Delhi, Q51, R15, pp1049-1074, 1979.

[7] MATSUMOTO T., YASUDA N., SAKAINO N. Dynamic property testing of coarse-grain materials using a large cyclic triaxial tester, *Civil Engineering Research Documents of the Ministry of Construction,* No. 2146, 1984

[8] WATANABE, H., BABA, K. A study on sliding stability evaluation method based on dynamic analysis of fill dams, *Large Dams,* No.97, pp.25-38, 1981 (in Japanese)

[9] Committee on the strengthening technology of Murayama dam and reservoir. Murayama Reservoir Maintenance Committee Report., 2002